# Tuning the magnetic, oxidation state and coordination behaviour of Iron and Cobalt Complexes on O/S Variation in mono-thio and dithio-oxamide chelating ligands

Luca Pilia, Davide Espa, Giorgio Concas, Francesco Congiu, Luciano Marchiò, Maria Laura Mercuri,
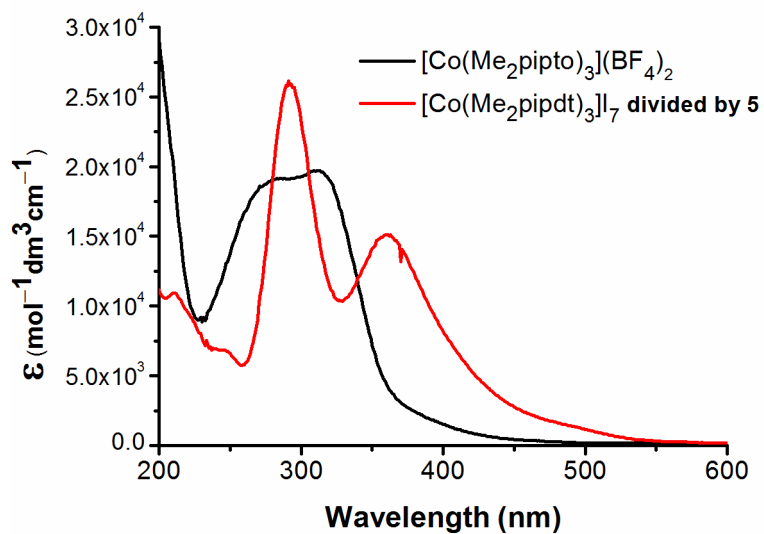
Angela Serpe and Paola Deplano

Supplementary Material

Me₂pipto E = −5.522 eV E = −1.631 eV

Me₂pipdt E = − 5.278 eV E = −1.932 eV

HOMO LUMO
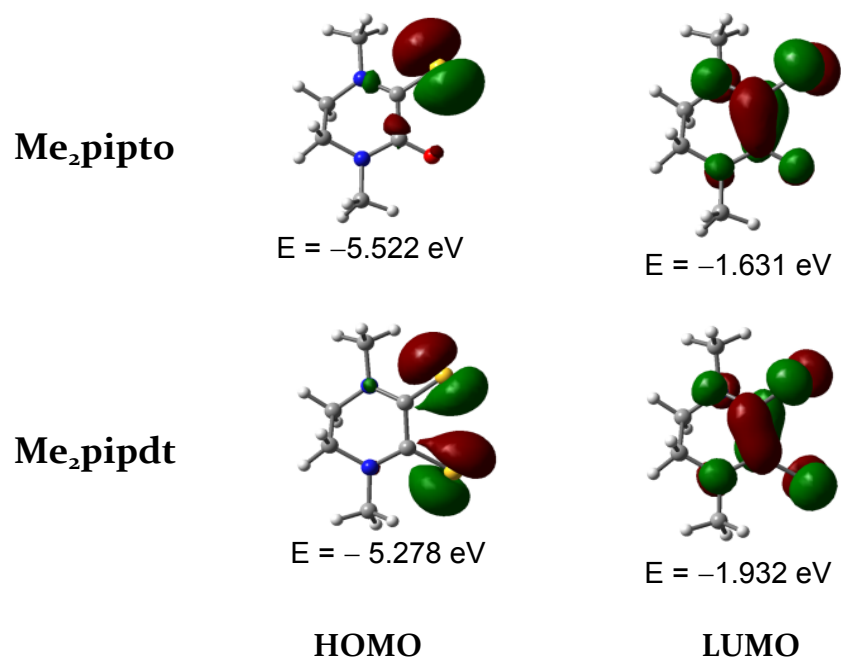
Figure S1. Drawing of HOMO and LUMO of Me$_2$pipto and Me$_2$pipdt ligands; the isosurfaces contour value is 0.04 and the energies are reported in electronvolts.
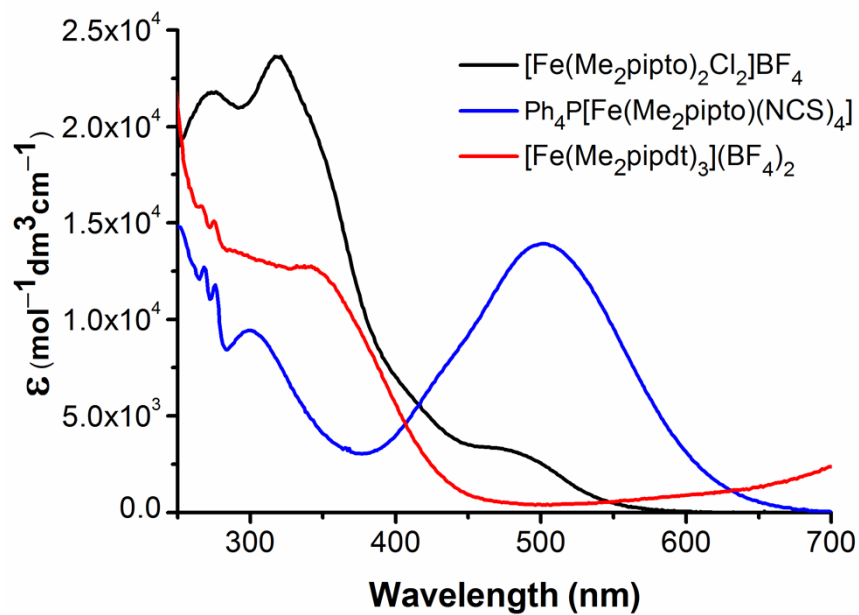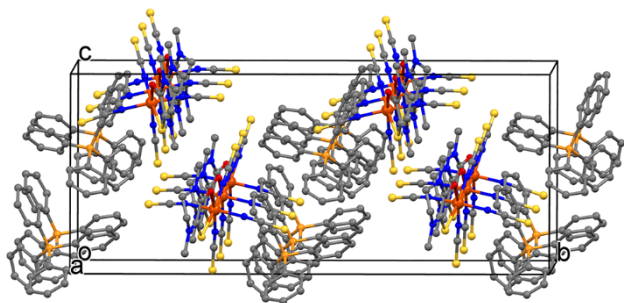

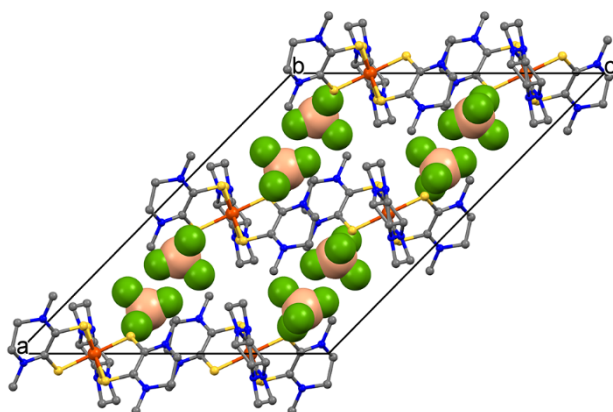**Figure S2**. UV-vis spectra of complexes **1**, **4** and **5** in CH$_3$CN solution.

**Figure S3**. UV-vis spectra of complexes **3** and **7** in CH$_3$CN solution.
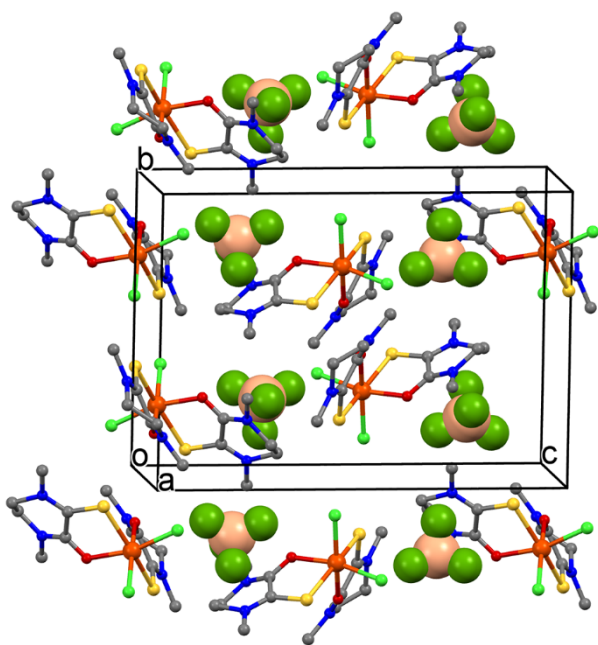
Figure S4. Crystal packing of [Fe(Me$_2$pipto)$_2$Cl$_2$]BF$_4$ (**1**) projected along the *a* axis.

Figure S5. Crystal packing of $Ph_4P[Fe(Me_2pipto)(NCS)_4]$ (**4**) projected along the *a* axis. The packing comprises alternate layers of complex molecules and PPh_4^+ cations

Figure S6. Crystal packing of $[Fe(Me_2pipdt)_3](BF_4)_2$ (**5**) projected along the *b* axis. The packing consists of layers of complex molecules with embedded BF_4^- anions.
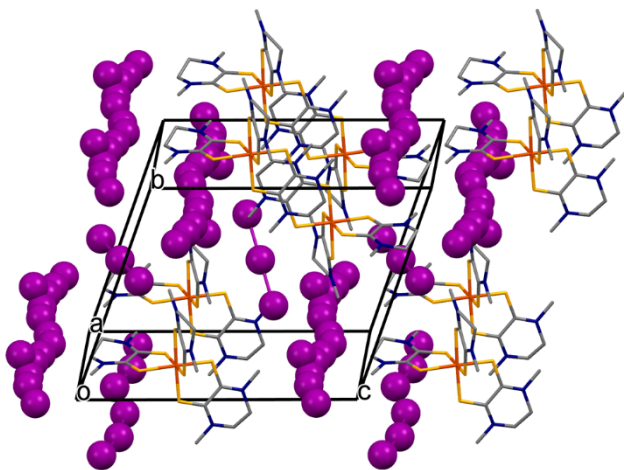
Figure S7. Crystal packing of $[Fe(Me_2pipdt)_3](I_3)_{1.8}(I)_{0.2}$ (**6**) projected along the *a* axis. Iodine atoms are depicted as purple spheres whereas the complex $[Fe(pipdt)_3]^{3+}$ in stick representation. Structural channels containing disordered iodine-based fragments run parallel to the *a* axis.
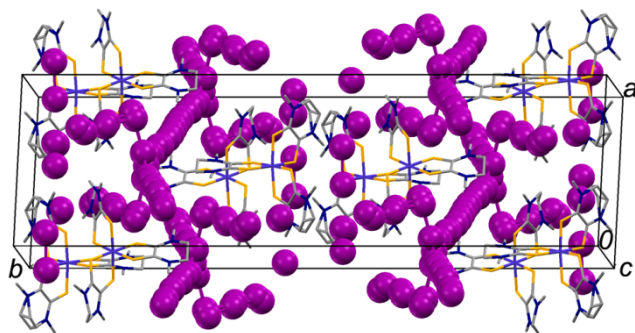
Figure S8. Crystal packing of $[Co(pipdt)_3]_2(I_3)_2(I)_4 \cdot 2I_2$ (**7**) projected along the *c* axis. Iodine atoms are depicted as purple spheres whereas the complex $[Co(pipdt)_3]^{3+}$ in stick representation. Structural channels containing disordered iodine-based fragments run parallel to the *c* axis.
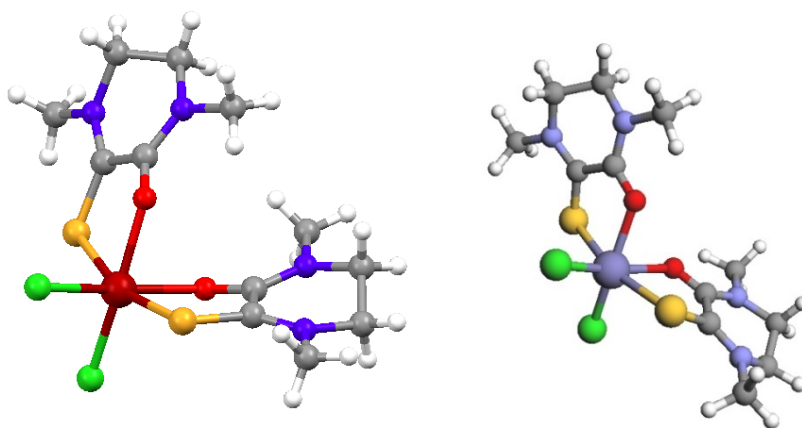
Figure S9. Comparison between the X-ray (left) and B3LYP/6-31G(d) calculated (right) structures of complex **1**.

Table S1. Comparison between experimental and *calculated*[a] bond lengths (Å) and angles (°) for **1**.

Fe-S(11)	2.5022(7)/*2.585*	S(11)-Fe-O(21)	78.13(4)/ *75.90*
Fe-S(12)	2.4595(6)/*2.585*	S(11)-Fe-Cl(2)	88.26(2)/*90.17*
Fe-O(21)	2.101(1)/ *2.151*	S(11)-Fe-Cl(1)	101.78(3)/*98.38*
Fe-O(22)	2.071(2)/ *2.151*	S(11)-Fe-S(12)	163.30(2)/*165.98*
Fe-Cl(1)	2.2699(7)/*2.224*	S(12)-Fe-O(22)	80.08(4)/*75.90*

5

Fe-Cl(2)	2.2592(6)/*2.224*	S(12)-Fe-O(21)	87.37(4)/*93.21*
C(11)-S(11)	1.675(2)/*1.680*	S(12)-Fe-Cl(2)	105.15(3)/*98.38*
C(21)-O(21)	1.248(2)/*1.245*	S(21)-Fe-Cl(1)	87.13(2)/*90.15*
C(12)-S(12)	1.679(2)/*1.680*	O(22)-Fe-Cl(2)	93.53(5)/*89.15*
C(22)-O(22)	1.258(2)/*1.245*	O(21)-Fe-Cl(2)	165.22(4)/*161.51*
C(11)-C(21)	1.510(3)/*1.526*	O(22)-Fe-Cl(1)	166.04(4)/*161.58*
C(12)-C(22)	1.508(3)/*1.526*	O(21)-Fe-Cl(1)	93.23(5)/*89.16*
		O(21)-Fe-O(22)	80.72(6)/*79.72*
S(11)-Fe-O(22)	89.35(5)/*93.23*	Cl(1)-Fe-Cl(2)	95.19(2)/*105.09*

[a] Calculated using 6-31G(d) as basis set.

Table S2. Comparison of experimental and calculated[a] high and low spin configurations bond lengths (Å) for **1**.

Bond	Experimental	B3LYP HS	OLYP HS	B3LYP LS	OLYP LS
Fe-S(11)	2.5022	2.585	2.608	2.389	2.288
Fe-S(12)	2.4595	2.585	2.608	2.389	2.288
Fe-O(21)	2.101	2.151	2.225	1.989	1.981
Fe-O(22)	2.071	2.151	2.225	1.989	1.981
Fe-Cl(1)	2.2699	2.224	2.223	2.227	2.226
Fe-Cl(2)	2.2592	2.224	2.223	2.227	2.226

[a] Calculated using 6-31G(d) as basis set.

Table S3. Comparison of experimental and B3LYP calculated[a] *high* and **low** spin configurations bond lengths (Å) and angles (°) for **2**.

Fe-S(11)	2.5022/*2.585*/**2.389**	S(11)-Fe-O(21)	78.13/*75.90*/**82.54**
Fe-S(12)	2.4595/*2.585*/**2.389**	S(11)-Fe-Cl(2)	88.26/*90.17*/**92.06**
Fe-O(21)	2.101/*2.151*/**1.989**	S(11)-Fe-Cl(1)	101.78/*98.38*/**93.40**
Fe-O(22)	2.071/*2.151*/**1.989**	S(11)-Fe-S(12)	163.30/*165.98*/**171.91**
Fe-Cl(1)	2.2699/*2.224*/**2.227**	S(12)-Fe-O(22)	80.08/*75.90*/**82.59**
Fe-Cl(2)	2.2592/*2.224*/**2.227**	S(12)-Fe-O(21)	87.37/*93.21*/**91.81**
C(11)-S(11)	1.675/*1.680*/**1.686**	S(12)-Fe-Cl(2)	105.15/*98.38*/**93.34**
C(21)-O(21)	1.248/*1.245*/**1.253**	S(21)-Fe-Cl(1)	87.13/*90.15*/**92.11**
C(12)-S(12)	1.679/*1.680*/**1.686**	O(22)-Fe-Cl(2)	93.53/*89.15*/**87.32**
C(22)-O(22)	1.258/*1.245*/**1.253**	O(21)-Fe-Cl(2)	165.22/*161.51*/**174.20**
C(11)-C(21)	1.510/*1.526*/**1.517**	O(22)-Fe-Cl(1)	166.04/*161.58*/**174.29**
C(12)-C(22)	1.508/*1.526*/**1.517**	O(21)-Fe-Cl(1)	93.23/*89.16*/**87.32**
		O(21)-Fe-O(22)	80.72/*79.72*/**90.70**
S(11)-Fe-O(22)	89.35(5)/*93.23*/**91.65**	Cl(1)-Fe-Cl(2)	95.19/*105.09*/**95.15**

[a] Calculated using 6-31G(d) as basis set.

Table S4. Comparison of experimental and OLYP calculated[a] *high* and **low** spin configurations bond lengths (Å) and angles (°) for **2**.

Fe-S(11)	2.5022/*2.608*/**2.288**	S(11)-Fe-O(21)	78.13/*74.52*/**83.63**
Fe-S(12)	2.4595/*2.608*/**2.288**	S(11)-Fe-Cl(2)	88.26/*90.86*/**87.71**
Fe-O(21)	2.101/*2.225*/**1.981**	S(11)-Fe-Cl(1)	101.78/*99.57*/**91.01**
Fe-O(22)	2.071/*2.225*/**1.981**	S(11)-Fe-S(12)	163.30/*162.83*/**178.03**
Fe-Cl(1)	2.2699/*2.223*/**2.226**	S(12)-Fe-O(22)	80.08/*74.52*/**83.62**
Fe-Cl(2)	2.2592/*2.223*/**2.226**	S(12)-Fe-O(21)	87.37/*92.12*/**97.83**
C(11)-S(11)	1.675/*1.681*/**1.690**	S(12)-Fe-Cl(2)	105.15/*99.57*/**91.01**
C(21)-O(21)	1.248/*1.248*/**1.268**	S(21)-Fe-Cl(1)	87.13/*90.86*/**87.71**
C(12)-S(12)	1.679/*1.681*/**1.690**	O(22)-Fe-Cl(2)	93.53/*89.37*/**89.22**
C(22)-O(22)	1.258/*1.248*/**1.268**	O(21)-Fe-Cl(2)	165.22/*160.99*/**168.60**
C(11)-C(21)	1.510/*1.528*/**1.491**	O(22)-Fe-Cl(1)	166.04/*160.99*/**168.59**
C(12)-C(22)	1.508/*1.528*/**1.491**	O(21)-Fe-Cl(1)	93.23/*89.37*/**89.23**
		O(21)-Fe-O(22)	80.72/*79.30*/**84.64**
S(11)-Fe-O(22)	89.35(5)/*92.12*/**97.84**	Cl(1)-Fe-Cl(2)	95.19/*105.27*/**98.36**

[a] Calculated using 6-31G(d) as basis set.

Table S5. Atomic Mulliken spin densities and relative energies of $[Fe(Me_2pipto)_2Cl_2]^+$ in doublet and sextet spin states.[a]

Functional	Configuration	Fe	O	S	Cl	Relative Energy
B3LYP	High Spin	3.8838	0.0397	0.1552	0.3308	
			0.0397	0.1552	0.3309	0 kJmol⁻¹
	Low Spin	1.0742	−0.0027	−0.0393	0.0048	
			−0.0026	−0.0396	0.0053	99.85 kJmol⁻¹
OLYP	High Spin	3.7284	0.0366	0.1714	0.3900	
			0.0366	0.1714	0.3901	0 kJmol⁻¹
	Low Spin	1.0383	0.0001	−0.0223	0.0561	
			0.0001	−0.0222	0.0561	94.45 kJmol⁻¹

[a] Basis set 6-311+G(d,p).

Table S6. Atomic Mulliken spin densities and relative energies of $[Co(Me_2pipto)_3]^{2+}$ in doublet and quartet spin states.[a]

Functional	Configuration	Co	O	S	Relative Energy
B3LYP	High Spin	2.6738	0.0053	0.0532	
			0.0178	0.1033	
			0.0291	0.0619	0 kJmol⁻¹
	Low Spin	1.0197	0.0139	−0.0073	
			0.0135	−0.0066	
			0.0051	−0.0194	61.72 kJmol⁻¹
OLYP	High Spin	2.5144	0.0132	0.0946	
			0.0506	0.1316	
			0.0310	0.1484	0 kJmol⁻¹
	Low Spin	1.0558	0.0292	−0.0024	
			0.0289	−0.0004	
			0.0087	−0.0085	7.57 kJmol⁻¹

[a] Basis set 6-311+G(d,p).